INTERNATIONAL JOURNAL OF AUTOMOTIVE SCIENCE AND TECHNOLOGY

2026, VOL. 10, NO:2, 350-369 www.ijastech.org e-ISSN: 2587-0963

Integrated Assessment of Non-Edible Biodiesel Production and Engine Performance and Emission Landscape under Diesel/Biodiesel Blends via RSM

Arif Savaş [1*] and Samet Uslu [2]

[1.] *Marine Engineering Department, Faculty of Maritime, Bandırma Onyedi Eylul University, Balıkesir, 10200, Turkey*
[2.] *Mechanical Engineering Department, Faculty of Engineering and Natural Sciences, Karabuk University, Karabuk, 78050, Turkey*

Abstract

Nowadays, a large portion of energy is produced using diesel engines. Although they have many benefits, like long lifespans, great efficiency, and dependability, they also have serious drawbacks, including the depletion of fossil fuel supplies and the release of pollutants that are bad for the environment and human health. The purpose of this study was to reduce these drawbacks and assess the viability of an environmentally acceptable, sustainable alternative fuel. Biodiesel fuels were used in this case because they may be utilized in current diesel engines with little to no modification. Cottonseed biodiesel was chosen among the various forms of biodiesel because of its high production potential and the fact that it is not intended for direct human use. In a single-cylinder, four-stroke diesel engine, fuel mixtures made by mixing cottonseed biodiesel with diesel fuel at volumetric percentages of 10%, 20%, 30%, and 40% were tested under six distinct engine loads and at a constant speed of 3000 rpm. According to the experimental results, CO and HC emissions significantly decreased as the biodiesel ratio rose, but CO_2 and NO_x emissions increased. Additionally, because biodiesel has a reduced calorific value, BSFC increased but BTE decreased. Optimization studies were conducted using three different scenarios with RSM and experimental data. In the scenario where all output parameters were assumed to be equally important, the ideal biodiesel ratio was found to be 9.22% and the engine load to be 1451.71 W. Under these ideal conditions, NO_x was 633.69 ppm, HC was 20.84 ppm, CO_2 was 5.27%, CO was 0.028%, BTE was 19.87%, and BSFC was 411.41 g/kWh. The outcomes show that cottonseed biodiesel is a sustainable and eco-friendly substitute fuel that, when used properly, can lower emissions in diesel engines.

Keywords: Cottonseed biodiesel; optimization; second generation biodiesel; transesterification

Research Article

History
Received 24.02.2026
Revised 28.03.2026
Accepted 13.05.2026

Contact
* Corresponding author
Arif Savaş
asavas@bandirma.edu.tr
Address: Marine Engineering Department, Faculty of Maritime, Bandırma Onyedi Eylul University, Balıkesir, Turkey
Tel:+902667170117

To cite this paper Savaş, A., Uslu, S. Integrated Assessment of Non-Edible Biodiesel Production and Engine Performance and Emission Landscape under Diesel/Biodiesel Blends via RSM. International Journal of Automotive Science and Technology. 2026; 10(3): 350-369. https://doi.org/10.30939/ijastech..1897071

1. Introduction

In the developing and modern world, the amount of energy required is always rising [1]. Sectors such as agriculture, industry, and transportation are among the highest energy consumers today [2]. Approximately 20% of the energy used today comes from the transportation industry. Internal combustion engines are typically used in this industry to produce energy [3]. Among internal combustion engines, diesel engines stand out with their high efficiency, longevity, and robustness [4]. These engines use fossil fuels to generate energy. Although diesel engines are indispensable due to their characteristics, fossil fuels pose significant problems for the future of diesel engines. The fact that fossil fuel reserves are located in specific regions, the depletion of reserves, and price fluctuations create anxiety about the future of fossil resources [5]. Furthermore, the combustion of fossil fuels in diesel engines produces emissions such as CO_2 and NO_x, which are harmful to human and environmental health [6,7]. Researchers have begun searching for new fuels to maintain the advantages of diesel engines while avoiding the disadvantages of fossil fuels.

Researchers have studied various alternative fuel types such as alcohols [8–10], ammonia [11], hydrogen [12], biogas [13], and biodiesel [14–16]. Among these fuels, biodiesel stands out as a significant alternative due to its advantages such as being usable in existing diesel engines without major modifications

[17], having a high oxygen content [18], and being sulphur-free [19]. Some studies conducted in this context are shown in Table 1.

Table 1. Literature review

Biodiesel	CO	HC	CO_2	NO_x	BSFC	BTE	Ref.
Palm biodiesel	↓	↓	↓	↑	↑	-	[20]
Levulinate	↓	↓	↑	↑	↑	-	[21]
Juliflora biodiesel	↓	↓	-	↑	↑	↓	[22]
Waste cooking biodiesel and Pongamia biodiesel	↓	↓	-	↑	↑	↓	[23]
mustard oil and pongamia pinnata oil	↓	↑	↓	↑	↑	-	[24]
spirulina microalgae	↓	↓	↑	↑	↑	↑	[25]
Waste plastic oil	↓	↓	↑	↑	↑	↓	[26]
Jojoba oil	↓	-	↑	↑	↑	↓	[27]
Eucalyptus oil	↓	↓	-	↑	↑	↓	[28]
Apricot seed kernel oil	↓	↓	↑	↑	↑	↑	[29]
Terebinth oil	↓	↓	↓	↑	↑	-	[30]

Previous studies have generally shown that the BSFC increases while BTE decreases due to the lower calorific value of cottonseed biodiesel. The high oxygen content and cetane number of biodiesels have contributed to reductions in CO and HC emissions; however, CO_2 and NO_x emissions typically increase with higher biodiesel content. Importantly, most studies evaluated biodiesel blends at discrete ratios and limited load conditions, and experiments were often terminated when significant performance deterioration or emission increases occurred. This approach has left several gaps in the literature: the effects of intermediate blend ratios on engine performance and emissions remain largely unexplored, nonlinear interactions between biodiesel fraction and engine load have not been systematically analyzed, and the optimal mixture ratios for balancing performance and emissions have not been identified. These limitations highlight the need for a more systematic and predictive approach, which can evaluate a wide range of blend ratios and operational conditions, providing actionable insights for optimizing both performance and emissions. Mathematical and statistical optimization techniques such as artificial neural network [31], response surface methodology (RSM) [32–34], machine learning [35] and Taguchi [36] allow for the determination of intermediate values using available experimental data. RSM is commonly chosen among these techniques because of its low error rate, minimal number of experiments required, and benefits for visualization.

Various studies have investigated the use of biodiesel produced from different feedstocks in diesel engines to improve sustainability and reduce emissions. Among these feedstocks, cottonseed oil stands out as a promising biodiesel source due to its high production potential, renewability, sustainability, and non-edible nature. The aim of this study is to comprehensively investigate the effects of cottonseed biodiesel–diesel blends on engine performance and emission characteristics and to determine the optimum operating conditions. Within the scope of the study, biodiesel was produced from cottonseed oil using the transesterification method and blended with diesel fuel at volumetric ratios of 10%, 20%, 30%, and 40% to obtain test fuels. Engine experiments were conducted at a constant speed of 3000 rpm under six different engine load conditions ranging from 500 to 3000 W. The experimental data were then analyzed using RSM to evaluate and optimize the effects of biodiesel ratio and engine load as input parameters on performance indicators, including BSFC and BTE, and emission parameters, including CO, HC, CO_2, and NO_x. While previous studies have explored biodiesel blends, engine performance, emissions, and RSM-based optimization, the novelty of the present study lies in its integrated approach: (i) conducting a wide-range experimental investigation over multiple load conditions, (ii) evaluating both performance and multiple emission parameters simultaneously, and (iii) developing predictive RSM models and performing multi-objective optimization under three weighting scenarios: equal weighting of performance and emission parameters (3:3), performance-priority weighting where performance parameters were assigned a weight of 3 and emission parameters a weight of 1, and emission-priority weighting where emission parameters were assigned a weight of 3 and performance parameters a weight of 1. This approach enables the identification of optimal operating conditions for cottonseed biodiesel blends under different operational priorities and provides practical insights for their efficient utilization as a sustainable alternative fuel.

2.Materials and Methods

2.1. Cottonseed biodiesel production

Biodiesel is a sustainable and renewable alternative fuel that can be made from a variety of basic sources [18]. Biodiesels are classified according to their raw materials. Biodiesels produced from sources used directly as food, such as sunflower, corn, and olive oil, are considered first-generation biodiesels [19]. Biodiesels produced from sources not used directly as food, such as jojoba [20], neem [21], and cottonseed [22], are called second-generation. Cottonseed has an annual production capacity of approximately 25 million tons [23]. This capacity, along with its sustainability, makes it a good alternative fuel. There are several ways to produce biodiesel, including as pyrolysis, transesterification, microemulsion creation, and dilution [37]. Transesterification is the most often used technique. This is the process by which triglyceride molecules combine with bases and alcohol to

create glycerol and fatty esters [38]. Figure 1 displays this method's chemical strategy.

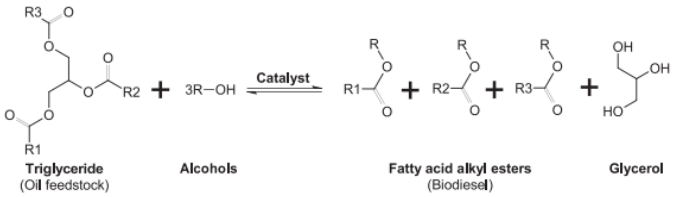


Figure 1. Transesterification

Cottonseed oil with high production potential that is grown in different places will be used in this investigation. Typically, cottonseed has about 25% oil [39]. Cottonseed oil was bought for this study from a nearby supplier. A simplified representation of the production of biodiesel is presented in Figure 2. Using a magnetic stirrer set at 800 rpm, cottonseed oil, which was bought from a local seller, was initially agitated for around 60 minutes at a temperature of 100–110°C in order to exclude impurities and water. To create the methoxide that would start the chemical reaction, methanol (CH_3OH) and sodium hydroxide (NaOH) were selected as the alcohols. A beaker containing methanol at a molar ratio of 6:1 and 1 weight percent NaOH was shaken at room temperature until the NaOH dissolved. Stirring started after adding the resultant combination and cooling the cottonseed oil to 60°C. The oil and methoxide combination was spun at 800 rpm at 60°C for sixty minutes. To extract the glycerine, the cottonseed biodiesel was stirred and then left in a separating funnel overnight. After the glycerine was extracted, the cottonseed methyl ester was purged with water at about 100°C to get rid of undesirable materials. Following the washing procedure, the biodiesel's surplus water was extracted at 800 rpm and a temperature of 100 to 110°C. Equation (1) was used to determine the biodiesel's efficiency [40]. A total of 1820 g of biodiesel was obtained from 2000 g of cottonseed oil during the production process. The operational efficiency was 91%.

$$Yield\ (\%) = \left(\frac{Cottonseed\ biodiesel\ (g)}{Cottonseed\ oil\ (g)}\right) * 100 \qquad (1)$$

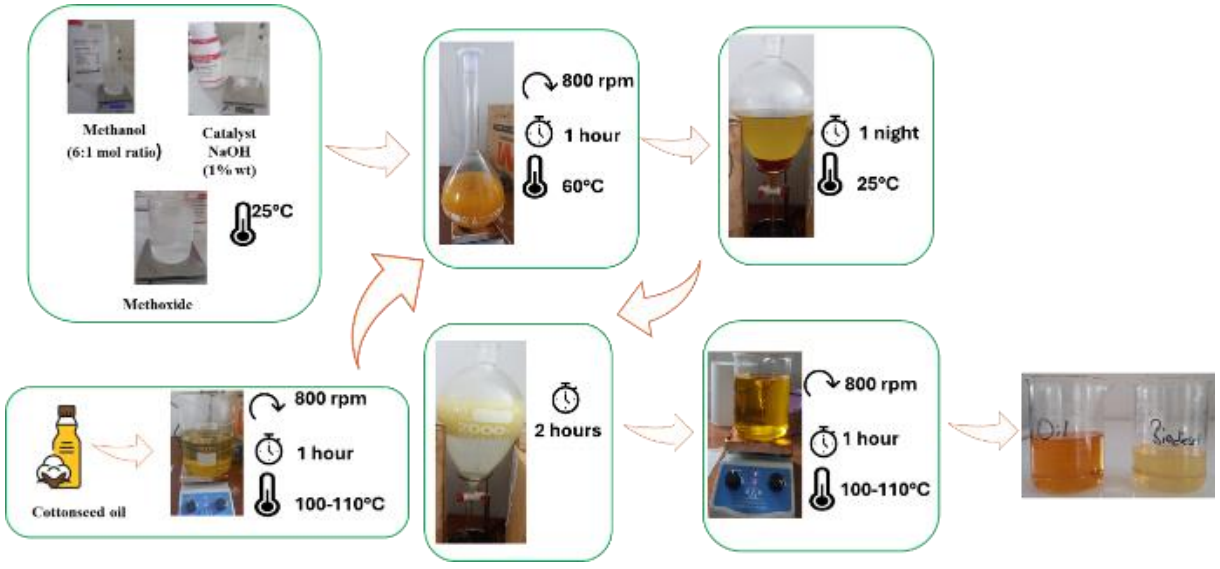


Figure 2. Cottonseed biodiesel production

The resulting biodiesel was used to make test fuels. 10%, 20%, 30%, and 40% by volume of cottonseed biodiesel were added to C0 (100% diesel) fuel, respectively. Figure 3illustrates the biodiesel addition schematically. The C10 (10% biodiesel + 90% diesel) test fuel was made by mixing 100 mL of cottonseed biodiesel with 900 mL of diesel in a beaker. A magnetic stirrer set to 800 rpm for two hours was then used to mix the fuels in this beaker to ensure even mixing. For the C20 (20% biodiesel + 80% diesel) test fuel, 800 mL of diesel and 200 mL of cottonseed biodiesel were added; for the C30 (30% biodiesel + 70% diesel), 700 mL of diesel and 300 mL of cottonseed biodiesel; and for the C40 (40% biodiesel + 60% diesel), 600 mL of diesel and 400 mL of cottonseed biodiesel. The characteristics of the test fuels used in the studies are displayed in Table 2.

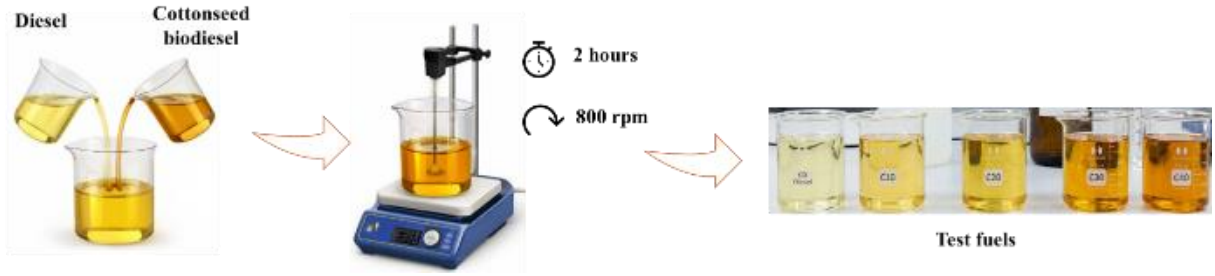


Figure 3. Biodiesel addition

Table 2. Characteristics of the test fuels

Properties	C0	C10	C20	C30	C40
Calorific value (MJ/kg)	45.846	45.270	44.694	44.117	43.541
Flash Point (◦C)	55	65.6	76.2	86.8	97.4
Density (kg/m^3 at 15 ◦C)	824.87	831.18	837.49	843.79	850.10
Kinematic viscosity (mm^2 /s at 40)	2.69	3.00	3.31	3.63	3.94

2.2 Experimental Process

For testing engine performance and exhaust pollutants, a single-cylinder, four-stroke diesel engine was utilized. The engine specs and emission device are shown in Table 3. The engine maintained a constant 3000 rpm during the experiment. A load device fitted with halogen lights was used to apply the load to the engine. To ensure that each experiment was conducted under the same conditions, the engine was given time to reach a stable operating state before measurements were taken. To lessen their detrimental effects on the environment, the studies were conducted in a controlled laboratory environment. The engine was initially run without any load to give it time to warm up and burn off any remaining old fuel. Following that, the engine was run at six distinct loads, ranging from 500 W to 3000 W. At each load, the engine was given time to stabilize. After engine stabilization, an emissions test probe was placed into the exhaust duct of the system to measure emissions. To be absolutely sure that all of the old fuel had been used up, the engine was run unloaded for ten minutes using only C0 fuel at the conclusion of each trial. The engine test setup is shown in Figure 4. All engine experiments were conducted in triplicate to ensure precision and reproducibility. Prior to testing, all measuring devices were carefully calibrated. The uncertainty for each measured parameter was determined based on the experimental data, resulting in ±1.20, ±1.30, ±1.20, ±2.16, ±0.90, ±0.60, and ±0.79 for CO, CO_2, HC, NO_x, BSFC, BTE, and load, respectively. Overall experimental uncertainty was estimated using a simplified root-sum-square (RSS) aggregation of the individual instrument measurement uncertainties. Specifically, the uncertainties associated with the measured parameters were combined to obtain an approximate overall experimental uncertainty, as presented in Equation (2). Based on this approach, the overall uncertainty of the experimental setup was determined to be ±3.32%.

This simplified RSS method provides an approximate estimate of cumulative measurement uncertainty under the assumption that individual uncertainty sources are independent. However, it should be noted that this approach does not account for covariance effects among combustion-related response variables and therefore represents an approximate uncertainty estimate rather than a full uncertainty propagation analysis. Nevertheless, the adopted method provides a practical assessment of measurement reliability and supports the overall repeatability and consistency of the experimental results.

$$U_{overall} = \sqrt{\begin{matrix}[(U_{BSFC})^2 + (U_{Load})^2 \\ +(U_{BTE})^2 + (U_{NO_x})^2 \\ +(U_{CO_2})^2 + (U_{HC})^2 + (U_{CO})^2]\end{matrix}} \quad (2)$$

Table 3. Engine and emission device

Emission device		
Parameter	**Accuracy**	**Measurement Range**
NO_x	± 1 ppm	0-5000 ppm
HC		0-10000 ppm
CO	0.01%	0 - 10% vol
CO_2		0 - 20% vol
Engine		
Model	Lutian 3GF-ME	
Number of Cylinder	Single	
Rated Power	3200W @ 3000 rpm	
Swept Volume	296 cm^3	

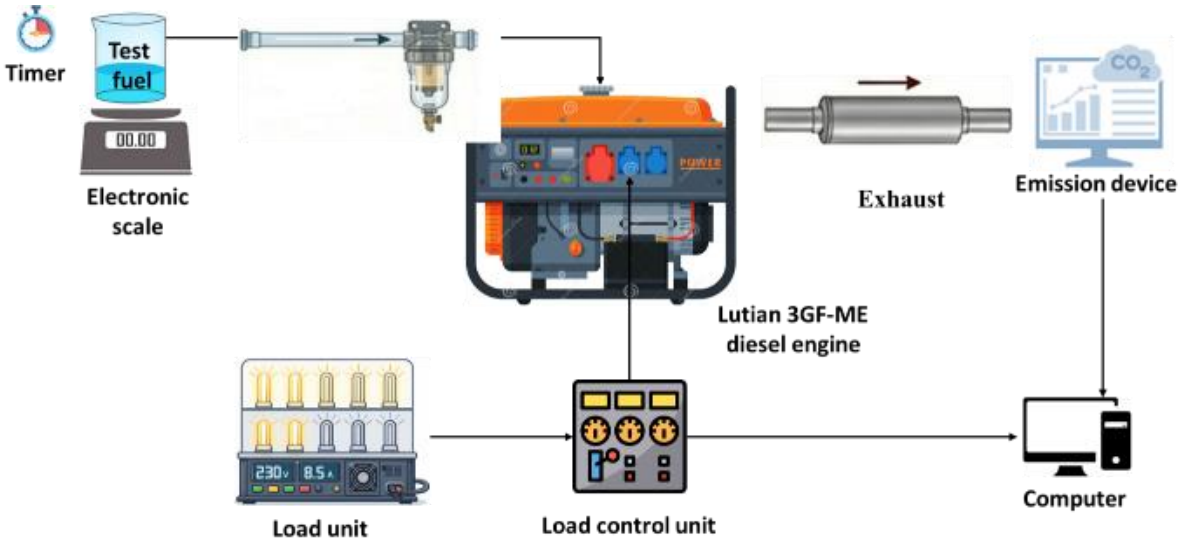


Figure 4. Engine test setup

2.3. Optimization

In 1951, K. B. Wilson and George E. P. Box introduced RSM. It tackles problems in an empirical model using mathematical and statistical techniques [41]. One of the many technical fields that uses RSM is internal combustion engines. Among the main features that distinguish RSM from other methods are its low error rate and the fact that it necessitates fewer experiments. RSM is used to determine the impacts and levels of influence of input parameters on parameters that are thought of as output parameters [42]. A second-order polynomial model was chosen to accurately capture the nonlinear behaviors and interaction effects found in diesel engine performance and emission characteristics. The adequacy of this model form was statistically validated using ANOVA, and it was preferred due to the significance of the second-order terms and high R^2, resulting in superior predictive ability compared to first-order models.[43,44]. CO, HC, CO_2, NO_x, BSFC, and BTE were identified as output parameters in this study, whereas the biodiesel ratio and engine load were identified as input parameters. The research was car-

ried out at a 95% confidence level, and the independent variables were automatically coded by Design-Expert software to ensure proper normalization and numerical stability during regression modeling. Regression coefficients were initially estimated in the coded variable space, but for practical interpretation, the final equations were expressed in terms of the actual experimental variables (biodiesel ratio and engine load).

RSM was employed to develop predictive models and optimize the effects of biodiesel ratio and engine load on engine performance and emission characteristics. The experimental design matrix was constructed to comprehensively cover the selected operating ranges of the input parameters while ensuring stable and repeatable engine operation under all test conditions. Biodiesel ratio and engine load were selected as the independent variables, and their corresponding levels are presented in Table 4. A total of 30 distinct experimental operating points, representing all combinations of the selected biodiesel ratios and load levels, were included in the RSM analysis. Each experimental condition was tested in triplicate to improve measurement reliability and reduce experimental uncertainty, and the mean values were used for statistical modeling.

The expanded experimental matrix provides sufficient coverage of the design space and adequate degrees of freedom for reliable development of polynomial regression models within the RSM framework. This comprehensive dataset enables robust evaluation of both the individual and interactive effects of biodiesel ratio and engine load on the studied responses. The use of a full-factorial experimental matrix encompassing all predefined factor-level combinations improves model robustness and enhances the statistical reliability of the subsequent ANOVA and optimization analyses. Table 4 lists the input parameter levels, and Table 5 presents the complete experimental design matrix together with the measured response values used for RSM modeling and optimization.

Table 4. Levels of the input parameters

	Biodiesel ratio (%)	Load (W)
Levels	0	500
	10	1000
	20	1500
	30	2000
	40	2500
	-	3000

2.4. Limitations of the Study

Although the present study provides valuable insights into the effects of biodiesel ratio and engine load on engine performance and emission characteristics, several limitations should be acknowledged. The experiments were conducted using a single biodiesel feedstock and a single-cylinder diesel engine under constant engine speed conditions. In addition, the engine tests were performed over relatively short operating periods under controlled laboratory conditions. Therefore, the obtained results may vary under different engine configurations, varying engine speeds, longer operating durations, or when different biodiesel feedstocks are used. Future studies may include multi-cylinder engines, variable speed operating conditions, longer-term engine tests, and different biodiesel feedstocks in order to further evaluate the applicability of biodiesel blends in diesel engines.

3. Results and Discussion

3.1. Experimental Results

Incomplete combustion is typically the cause of CO emissions. The change in CO emissions with regard to engine load and biodiesel percentage is depicted in Figure 5. Emissions in all test fuels rose after a certain load because there was not enough time for full combustion, but they decreased up to that point. With C30 test fuel, the lowest CO emission value was 0.015% at 2500 W load, while with C40 test fuel, the highest CO emission value was 0.081% at 500 W load. For C10, C20, and C30 test fuels, CO emission levels were 21.15%, 25.88%, and 26.77% lower than C0 fuel, respectively, however for C40 test fuel, they were 23.58% higher. Biodiesels' high oxygen content enhances combustion, promoting full combustion and lowering CO emissions [45]. However, as the biodiesel ratio rises, fuel viscosity rises as well, disrupting fuel atomization and increasing incomplete combustion [46]. Incomplete combustion is causing an increase in CO emissions [47]. According to the optimization study, fuel with 10–30% biodiesel added by volume to diesel at a load of about 2000–2500 W had the lowest CO emissions.

2.4. Limitations of the Study

Although the present study provides valuable insights into the effects of biodiesel ratio and engine load on engine performance and emission characteristics, several limitations should be acknowledged. The experiments were conducted using a single biodiesel feedstock and a single-cylinder diesel engine under constant engine speed conditions. In addition, the engine tests were performed over relatively short operating periods under controlled laboratory conditions. Therefore, the obtained results may vary under different engine configurations, varying engine speeds, longer operating durations, or when different biodiesel feedstocks are used. Future studies may include multi-cylinder engines, variable speed operating conditions, longer-term engine tests, and different biodiesel feedstocks in order to further evaluate the applicability of biodiesel blends in diesel engines.

3. Results and Discussion

3.1. Experimental Results

Incomplete combustion is typically the cause of CO emissions. The change in CO emissions with regard to engine load and biodiesel percentage is depicted in Figure 5. Emissions in all test fuels rose after a certain load because there was not enough time

for full combustion, but they decreased up to that point. With C30 test fuel, the lowest CO emission value was 0.015% at 2500 W load, while with C40 test fuel, the highest CO emission value was 0.081% at 500 W load. For C10, C20, and C30 test fuels, CO emission levels were 21.15%, 25.88%, and 26.77% lower than C0 fuel, respectively, however for C40 test fuel, they were 23.58% higher. Biodiesels' high oxygen content enhances combustion, promoting full combustion and lowering CO emissions [45]. However, as the biodiesel ratio rises, fuel viscosity rises as well, disrupting fuel atomization and increasing incomplete combustion [46]. Incomplete combustion is causing an increase in CO emissions [47]. According to the optimization study, fuel with 10–30% biodiesel added by volume to diesel at a load of about 2000–2500 W had the lowest CO emissions.

Table 5. Experimental design matrix and measured responses used for RSM analysis

Biodiesel Ratio (%)	Load (W)	CO (%)	HC (ppm)	CO_2 (%)	NOx (ppm)	BSFC (g/kWh)	BTE (%)
0	500	0.073	7	4.220	378	877.16	8.95
0	1000	0.044	17	4.611	450	494.00	16.54
0	1500	0.036	24	5.225	556	373.33	21.03
0	2000	0.033	30	6.122	690	336.84	23.31
0	2500	0.037	35	7.368	843	310.28	25.31
0	3000	0.057	41	8.043	906	319.08	24.61
10	500	0.07	7	4.175	402	929.80	8.55
10	1000	0.043	16	4.435	467	502.18	15.84
10	1500	0.026	24	5.057	572	394.61	20.15
10	2000	0.02	29	6.081	725	356.01	22.34
10	2500	0.027	33	7.090	870	327.98	24.25
10	3000	0.042	38	8.169	930	337.50	23.56
20	500	0.067	6	4.380	456	941.02	8.56
20	1000	0.039	15	4.516	550	508.51	15.84
20	1500	0.032	21	5.15	639	399.7395	20.15
20	2000	0.023	25.56	6.193	783	360.7087	22.33
20	2500	0.019	31.06	7.241	931	332.2791	24.24
20	3000	0.031	33.73	8.239	989	341.7177	23.57
30	500	0.055	5	4.693	502	991.1594	8.23
30	1000	0.041	14.22	5.111	637	535.5791	15.24
30	1500	0.026	19.46	5.464	730	420.9064	19.39
30	2000	0.023	23.05	6.422	880	379.8279	21.48
30	2500	0.025	28.06	7.863	984	349.6312	23.34
30	3000	0.035	31.44	8.697	1036	359.168	22.72
40	500	0.081	9.41	3.952	356	1031.561	8.02
40	1000	0.062	21.39	4.272	424	597	14.83
40	1500	0.051	25.98	4.972	517	438.212	18.87
40	2000	0.04	32.35	5.908	661	395.4699	20.91
40	2500	0.043	38.39	6.964	834	364.2071	22.70
40	3000	0.063	43.09	7.968	885	374.2301	22.09

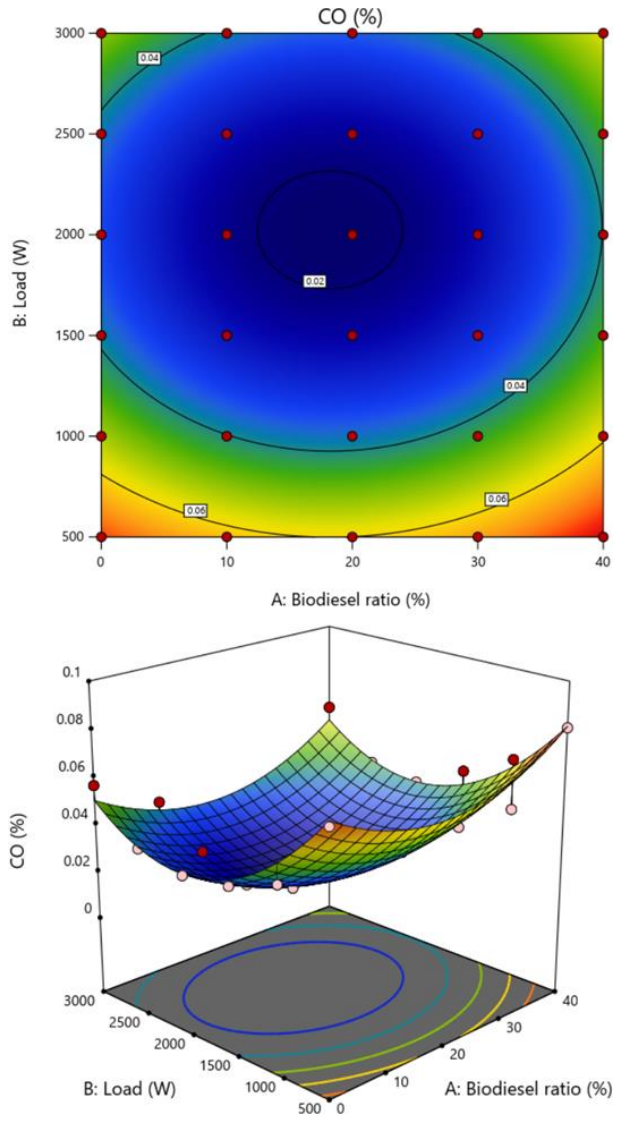


Figure 5. Response surface of CO emissions versus cottonseed biodiesel ratio and load

HC emissions are another byproduct of burning that is incomplete. A number of factors contribute significantly to HC emissions, including insufficient air-fuel ratio in the combustion chamber, poor design, wall cooling, weak atomization, and intake system flaws [48]. The change in HC emissions based on engine load and the biodiesel ratio is depicted in Figure 6. The minimum HC exhaust value was 5 ppm at 500 W load when using C30 test fuel, and the maximum HC emission value was 43 ppm at 3000 W load when using C40 test fuel. In all test fuels, HC emissions rose as the load increased. While HC emissions rose by 14.56% for C40 test fuel, they fell by 5.73%, 13.76%, and 22.12% for C0, C10, and C20 test fuels, respectively, in comparison to C0 fuel. HC emissions decreased as a result of biodiesels' high cetane number [49]. Nevertheless, after a while, increasing the proportion of additional biodiesel made combustion poorer and increased HC emissions. The optimization investigation found that test fuel containing roughly 20% cottonseed biodiesel by volume produced the lowest HC emissions at low loads (about 500 W).

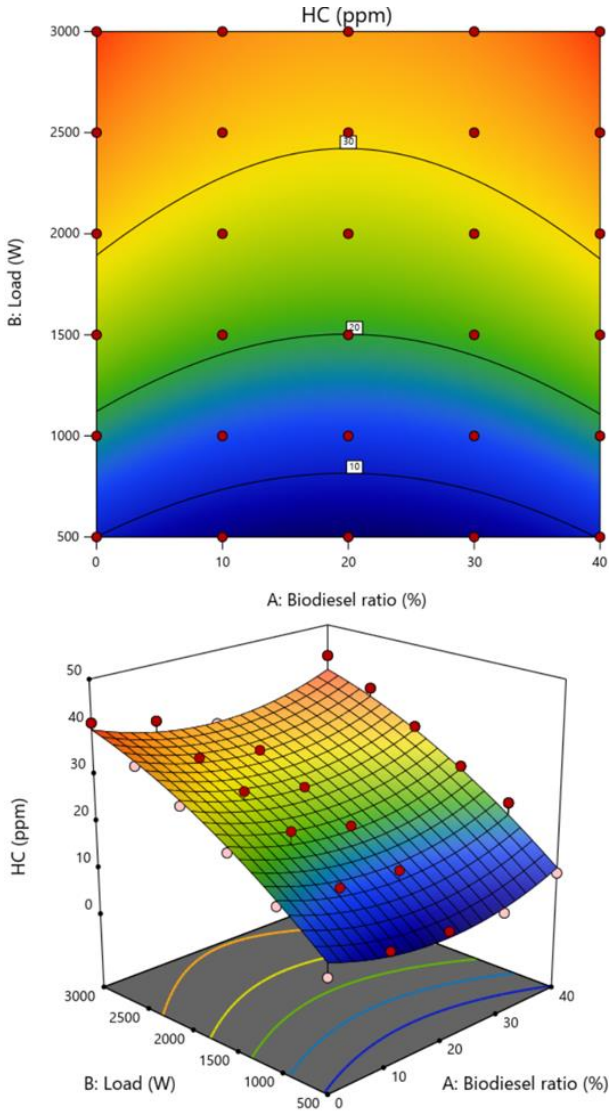


Figure 6. Response surface of HC emissions versus cottonseed biodiesel ratio and load

NO_x emissions, which are highly harmful to the environment and directly correspond with the temperature and pressure inside the cylinder, are produced when nitrogen in the air reacts with high temperatures and pressures inside the cylinder [50,51]. Figure 7 illustrates how NO_x emissions change based on engine load and the biodiesel percentage. NO_x emissions increased with increasing load in all test fuels. The C40 test fuel exhibited the minimal NO_x emission (356 ppm) and the C30 test fuel showed the greatest NO_x emission (1036 ppm) with a 500 W load. NO_x

values rose by 4.01%, 15.16%, and 27.40% for the C10, C20, and C30 test fuels, respectively, in comparison to the C0 test fuel, while they fell by 4.35% for the C40 test fuel. NO_x emissions rose as a result of higher in-cylinder temperature and pressure brought on by the enhanced combustion brought about by the high oxygen content of biodiesels. Increasing the proportion of biodiesel, however, increased fuel viscosity, which decreased NO_x emissions and combustion efficiency [52]. At low loads like 500 W, diesel fuels with 0-5% or 35-40% biodiesel added by volume showed the lowest NO_x emissions.

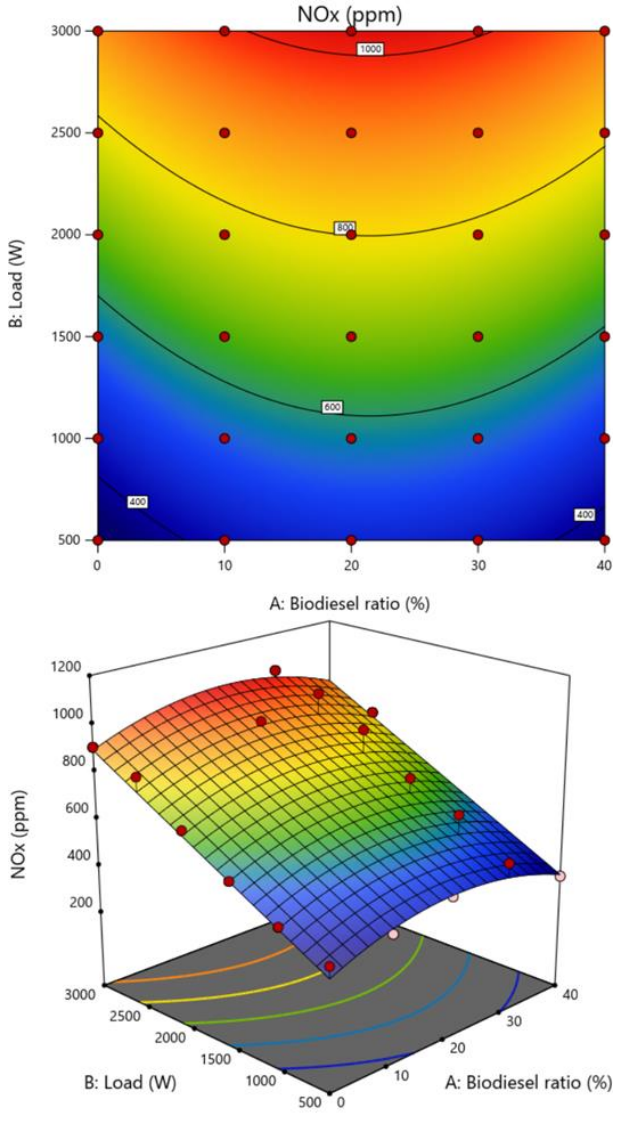


Figure 7. Response surface of NO_x emissions versus cottonseed biodiesel ratio and load

Internal combustion engines are the main source of greenhouse gas emissions, and CO_2 emissions are directly correlated with the fuel's carbon content and combustion efficiency. Understanding CO_2 emissions is crucial for assessing the total environmental impact of alternative fuels in engines powered by biodiesel [53]. Figure 8 exhibits how CO_2 emissions vary based on engine load and the biodiesel percentage. The C40 test fuel had the lowest CO_2 emission of all the test fuels at a load of 3000 W, measuring 3.962%, while the C30 test fuel had its greatest CO_2 emission figure, measuring 8.697%. As the load grew, CO_2 emissions rose for all test fuels. The CO_2 emission change for C10, C20, and C30 test fuels was 1.73%, 3.92%, and 7.73% higher than that of C0 fuel, respectively, but the CO_2 emission change for C40 test fuel was 4.74% lower. Because biodiesel has a high cetane number and produces more CO_2 emissions when it burns completely, adding it improved combustion [54]. Nevertheless, after a certain point, combustion degraded and CO_2 emissions declined as the biodiesel ratio increased.

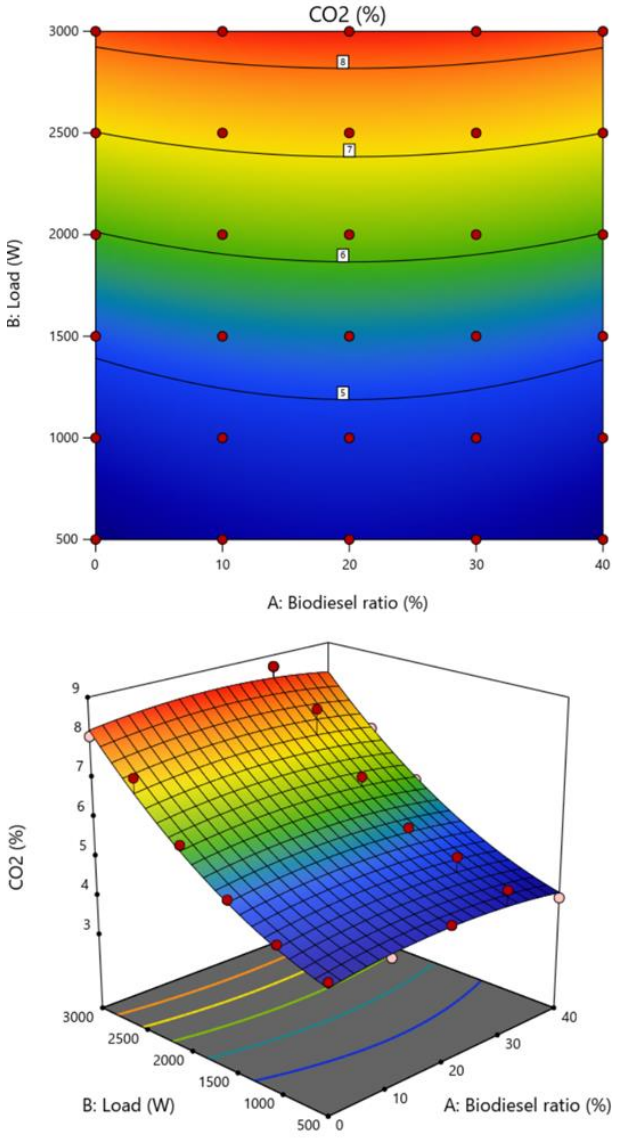


Figure 8. Response surface of CO_2 emissions versus cottonseed biodiesel ratio and load

With the study looking at different fuel types and their effects, BSFC is one of the important engine properties. The density, viscosity, and calorific value of the fuel are all strongly connected with this metric, which indicates how many grams of fuel are required to produce one kW of load in an hour [55]. The BSFC change based on engine load and biodiesel ratio is portrayed in Figure 9. With C0 fuel at a 2500 W load, the lowest BSFC value was 310 g/kWh; with C40 test fuel at a 500 W load, the highest BSFC value was 1032 g/kWh. Fuel consumption was high at low loads and decreased as the load increased for all test fuels. Fuel consumption was decreased and combustion efficiency was enhanced as cylinder temperature and pressure rose with increasing load [56]. However, after a certain load, non-homogeneous combustion and a lack of time for full combustion led to an increase in fuel consumption. The BSFC values for C10, C20, C30, and C40 fuels increased by 5.78%, 7.12%, 12.76%, and 17.41%, respectively, in comparison to C0 fuel. Because biodiesels often have a lower calorific value than diesel, more fuel is needed to provide the same amount of power [57]. Moreover, viscosity rises with increasing biodiesel percentage, decreasing combustion efficiency and raising BSFC [58]. The test fuel with 0–5% biodiesel added to diesel in the 2000–2500 W load range had the lowest BSFC value in the optimization research.

BTE, which indicates the amount of fuel energy converted to mechanical power, is a further significant engine performance indicator. The calorific value of the fuel, engine output power, and fuel consumption all affect this performance metric. Figure 10 explains how the amount of biodiesel and engine load affect BTE. With C40 test fuel, the lowest BTE value was determined to be 8% at 500 W load, while with C0 test fuel, the highest BTE value was determined to be 25% at 2500 W load. The BTE value was low at low loads and rose with increasing load in all test fuels. But after a certain load value, it dropped once more because there wasn't enough time for full combustion. The BTE values of the C10, C20, C30, and C40 fuels dropped by 4.25%, 5.27%, 7.84%, and 10.32%, respectively, in comparison to the C0 record. Biodiesel's high viscosity reduces combustion efficiency by interfering with fuel atomization. Moreover, the BTE value is lowered by the higher fuel use brought on by biodiesels' poor calorific value [59,60]. At loads between 2500 and 3000 W, the test fuel with 0-5% biodiesel by volume to diesel had the highest BTE value.

3.2. Optimization with RSM

The final reduced quadratic models for engine performance and emission responses (HC, CO_2, NOx, BSFC, and BTE) were developed using a systematic backward elimination procedure. In this process, statistically insignificant higher-order and interaction terms were iteratively removed. However, model reduction was not performed purely on the basis of statistical significance; instead, it was constrained by the hierarchy principle to preserve model structure and ensure physically meaningful relationships among linear, interaction, and quadratic terms. In this context, biodiesel ratio (A) and engine load (B) were treated as fundamental governing variables of the combustion system and were therefore retained in the model even when their individual statistical contributions were comparatively weak in certain responses, to ensure physical consistency and comparability across all response surfaces. The ANOVA results presented in Tables 6-11 summarize the effects of biodiesel ratio (A), engine load (B), their interaction (AB), and quadratic terms (A^2 and B^2) at a 95% confidence level. Within this framework, F-values were used to quantify the relative contribution of each term to response variability, while p-values were reported solely as indicators of statistical evidence rather than as the sole basis for term elimination. Accordingly, model interpretation was guided by a combined statistical–physical evaluation approach rather than a purely significance-driven selection strategy.

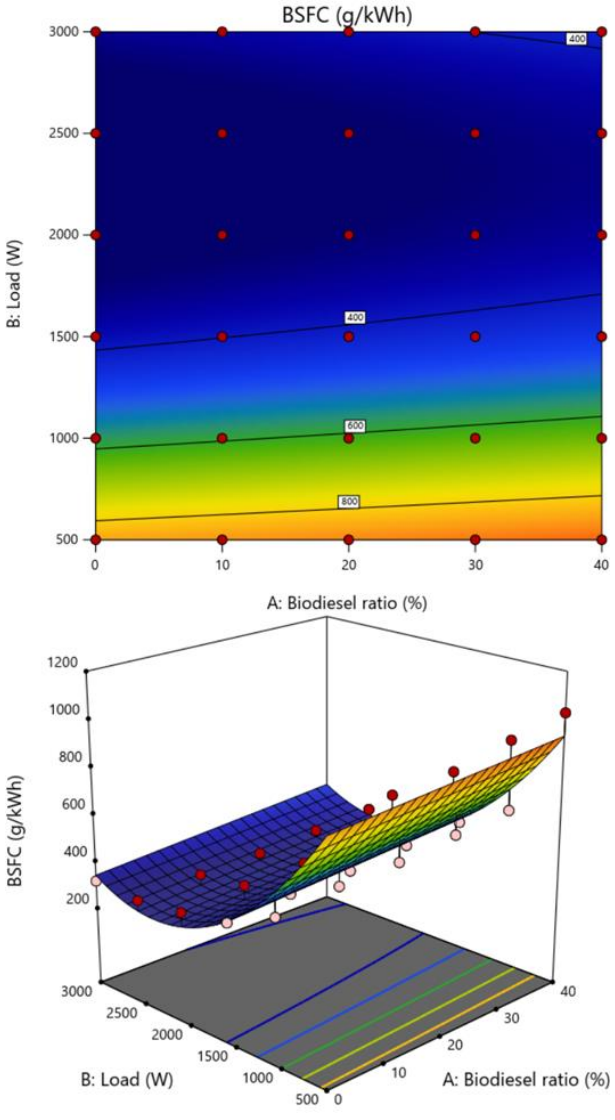


Figure 9. Response surface of BSFC emissions versus cottonseed biodiesel ratio and load

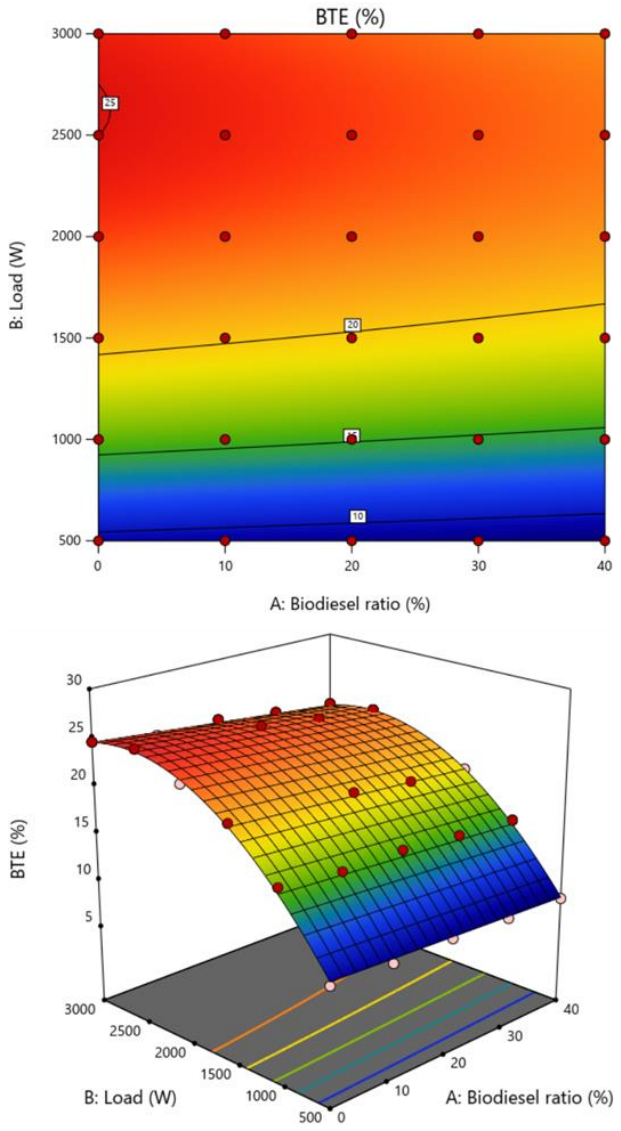


Figure 10. Response surface of BTE emissions versus cottonseed biodiesel ratio and load

For HC, CO_2, and NO_x models in particular, the observed insignificance of certain linear or interaction terms does not contradict model validity, as these variables were retained under hierarchical and physical constraint considerations to maintain model consistency and structural integrity. This approach avoids over-simplification of the response surfaces and ensures that all models remain comparable within a unified experimental design framework. Overall, the high Adeq Precision values, low C.V. %, strong R^2–Adjusted R^2–Predicted R^2 agreement, and statistically significant overall model F-values confirm that the developed reduced quadratic models provide a robust, stable, and physically consistent representation of the complex interactions between biodiesel blending ratio, engine load, and engine performance–emission characteristics.

Table 6. F-value and p-value of CO

	F-value	p-value
Model	17.63	< 0.0001
A-Biodiesel ratio	1.98	0.0226
B-Load	25.29	< 0.0001
A^2	7.59	< 0.0001
B^2	18.42	< 0.0001

Table 7. F-value and p-value of HC

	F-value	p-value
Model	90.68	< 0.0001
A-Biodiesel ratio	1.49	0.8674
B-Load	312.95	< 0.0001
A^2	13.81	< 0.0001
B^2	11.65	0.0024

Table 8 F-value and p-value of CO_2

	F-value	p-value
Model	77.94	< 0.0001
A-Biodiesel ratio	0.9186	0.9476
B-Load	355.66	< 0.0001
A^2	0.6549	0.0351
B^2	14.51	< 0.0001

Table 9. F-value and p-value of NO_x

	F-value	p-value
Model	38.33	< 0.0001
A-Biodiesel ratio	0.168	0.2270
B-Load	153.06	< 0.0001
A^2	5.83	< 0.0001

Table 10. F-value and p-value of BSFC

	F-value	p-value
Model	53.88	< 0.0001
A-Biodiesel ratio	1.64	0.0224
B-Load	98.65	< 0.0001
B^2	58.41	<0.0001

Table 11. F-value and p-value of BTE

	F-value	p-value
Model	1021.6	< 0.0001
A-Biodiesel ratio	46.34	< 0.0001
B-Load	2628.52	< 0.0001
AB	5.61	0.0385
B^2	528.67	<0.0001

To improve model parsimony and address statistically insignificant terms identified in the initial full quadratic models, backward elimination was applied to each response surface model. Terms with p-values greater than 0.05 were removed unless their retention was required to preserve hierarchical consistency. The statistical performance of the original full models

and the revised reduced models was compared using R^2, Adjusted R^2, and Predicted R^2 values, as presented in Table 12.

As shown in Table 12, model reduction caused negligible changes in R^2 values while generally improving or maintaining Adjusted R^2 and Predicted R^2 statistics. In particular, the Predicted R^2 values increased for all response variables following model reduction, indicating enhanced predictive capability and reduced overfitting. These results confirm that the reduced models provide a more parsimonious and statistically robust representation of the experimental data without compromising predictive accuracy.

The statistical adequacy of the developed quadratic models was evaluated using the performance metrics presented in Table 13. The Adeq Precision values, representing the signal-to-noise ratio, are substantially higher than the recommended threshold of 4 for all responses, confirming an adequate and reliable model signal. In addition, the low Coefficient of Variation (C.V. %) values indicate excellent repeatability and consistency of the experimental data, supporting the robustness of the experimental design.

The regression equations for all response variables are presented in both coded and actual forms in Table 14. In the initial formulation, the engine load variable in the actual equations was expressed in Watts (W), resulting in very small coefficient magnitudes (e.g., on the order of 10^{-5}–10^{-3} for load-dependent terms in CO, HC, CO_2, and BTE equations). Although these values are mathematically correct, such scaling reduces the direct interpretability of the coefficients from an engineering perspective, since a unit change in load (1 W) does not represent a physically meaningful variation in engine operation. To improve interpretability, the engine load variable was redefined in kilowatts (kW) in all actual-variable equations. This transformation preserves the mathematical structure of the models while eliminating scale compression, allowing the regression coefficients to reflect realistic variations in engine load. As a result, the influence of load on responses such as CO, HC, NO_x, BSFC, and BTE can be more clearly interpreted in practical terms. It is important to note that a high R^2, such as that obtained for the BTE model, indicates strong predictive agreement between experimental and estimated values; however, it does not, by itself, ensure the physical interpretability of individual regression coefficients. For this reason, both coded and actual-variable equations are provided. The coded equations are primarily used for statistical evaluation and identification of factor significance, whereas the actual equations (expressed in kW) support engineering interpretation and practical applicability. The actual-variable equations correspond to reduced regression models derived from coded-space analysis. During model reduction, statistically insignificant terms ($p > 0.05$) were removed while preserving hierarchical structure. Consequently, the final equations retain only the dominant contributions of biodiesel ratio (BR) and engine load, which govern the response behavior. The inclusion of both equation forms enables a comprehensive evaluation of the system from both statistical and physical perspectives.

The error rates between the optimization results and the experimental data were calculated using the actual regression equations. The biodiesel ratio (BR) and engine load (kW) values listed in Table 14 were substituted into the corresponding actual-variable regression models to obtain the predicted response values. The percentage error between the predicted and experimental values was then computed to evaluate the predictive performance of the developed models. The error distribution is illustrated in Figure 11. Among the investigated responses, the highest deviation was observed for BSFC with an error of 9.97%, while the lowest error was obtained for BTE with 2.02%, indicating a strong agreement between the experimental measurements and model predictions across all response parameters.

Table 12. Comparison of statistical performance metrics for full and reduced RSM models before and after model reduction

Response	Model	R^2	Adjusted R^2	Predicted R^2
CO	Full	0.9216	0.9053	0.8651
	Reduced	0.9209	0.9083	0.8801
HC	Full	0.9630	0.9553	0.9371
	Reduced	0.9614	0.9552	0.9439
CO_2	Full	0.9719	0.9661	0.9576
	Reduced	0.9719	0.9674	0.9612
NO_x	Full	0.9417	0.9296	0.9138
	Reduced	0.9417	0.9349	0.9257
BSFC	Full	0.9445	0.9329	0.9123
	Reduced	0.9351	0.9276	0.9139
BTE	Full	0.9946	0.9935	0.9919
	Reduced	0.9946	0.9937	0.9926

Table 13. Fit Statistics

	CO	HC	CO2	NOx	BSFC	BTE
Std. Dev.	0.0052	2.30	0.2667	53.32	59.94	0.4395
Mean	0.0421	24.10	5.95	686.10	487.36	18.90
C.V. %	12.23	9.53	4.48	7.77	12.30	2.33
R^2	0.9209	0.9614	0.9719	0.9417	0.9351	0.9946
Adjusted R^2	0.9083	0.9552	0.9674	0.9349	0.9276	0.9937
Predicted R^2	0.8801	0.9439	0.9612	0.9257	0.9139	0.9926
Adeq Precision	29.949	37.446	40.239	35.858	30.683	93.880

Table 14. Regression equations*

Response	Equation	Coded/ Actual
CO	$0.0199+0.0032\cdot A-0.0122\cdot B+0.0183\cdot A^2+0.0279\cdot B^2$	Coded Equation
	$0.1069-0.0017\cdot BR-0.01786\cdot Load+4.58\cdot 10^{-5}\cdot BR^2+0.01786\cdot Load^2$	Actual Equation
HC	$23.0657+0.1000\cdot A+14.8142\cdot B+5.3809\cdot A^2-3.5491\cdot B^2$	Coded Equation
	$0.6505-0.5331\cdot BR+19.8\cdot Load+0.0134\cdot BR^2-2.27\cdot Load^2$	Actual Equation
CO_2	$5.8034+0.0045\cdot A+2.0583\cdot B-0.2592\cdot A^2+0.5989\cdot B^2$	Coded Equation
	$3.832+0.0261\cdot BR+0.31\cdot Load-0.0007\cdot BR^2+0.383\cdot Load^2$	Actual Equation
iNO_x	$743.9809+17.0333\cdot A+282.6714\cdot B-115.7619\cdot A^2$	Coded Equation
	$215.4457+12.4278\cdot BR+226.1\cdot Load-0.2894\cdot BR^2$	Actual Equation
BSFC	$353.7515+37.5846\cdot A-258.2147\cdot B+286.3073\cdot B^2$	Coded Equation
	$1238.8299+1.8792\cdot BR-847.9\cdot Load+183.24\cdot Load^2$	Actual Equation
BTE	$21.4365-0.9649\cdot A+7.2375\cdot B-0.3630\cdot AB-5.4390\cdot B^2$	Coded Equation
	$1.1002-0.0228\cdot BR+18.2\cdot Load-1.452\cdot 10^{-2}\cdot BR\cdot Load-3.481\cdot Load^2$	Actual Equation

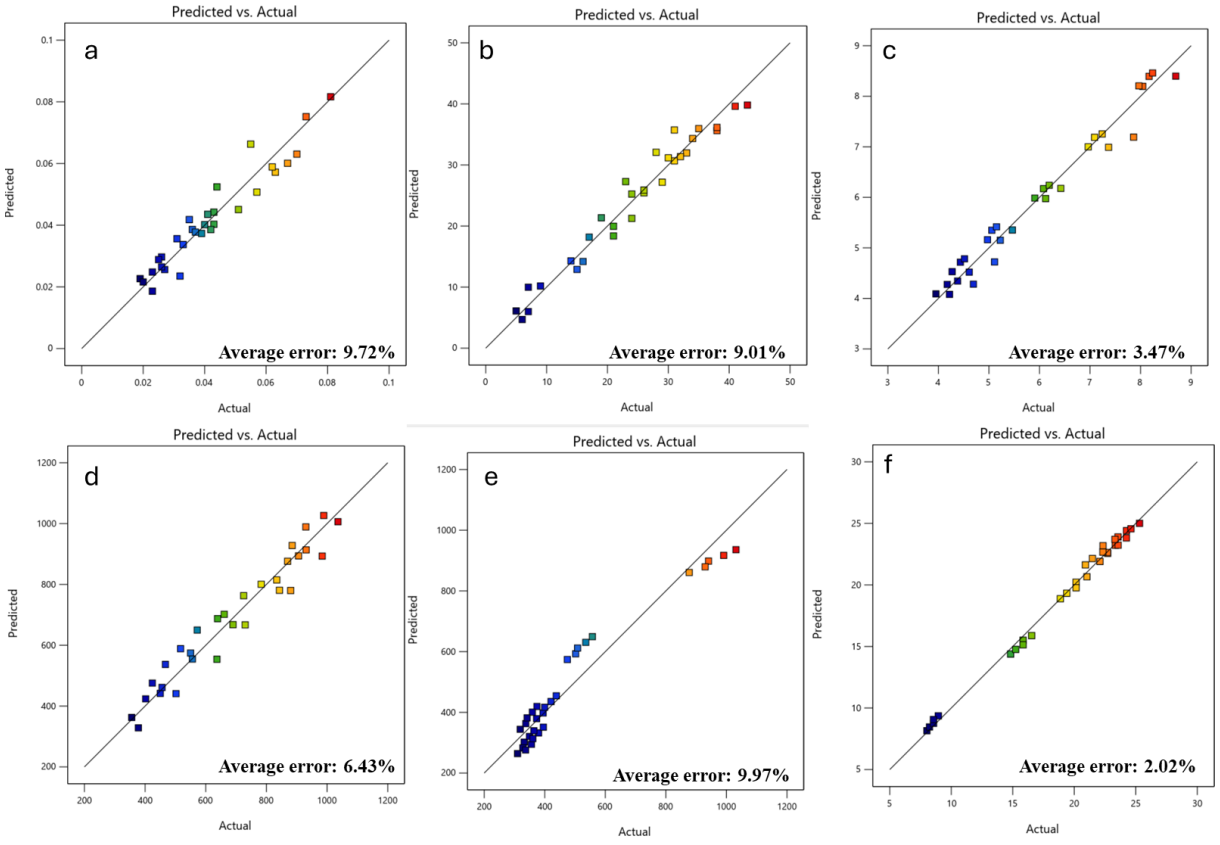


Figure 11. Error rates of a) CO b)HC c) CO_2 d)NO_x e)BSFC f)BTE

In order to address the assumption of equal importance among response variables, a sensitivity analysis was conducted using different weighting scenarios in the multi-objective optimization. Three scenarios were evaluated. In Scenario 1, equal importance was assigned to all response variables. In Scenario 2, emission parameters (NO_x, CO_2, HC, and CO) were given higher importance, while performance parameters (BTE and BSFC) were assigned lower importance. Conversely, in Scenario 3, performance parameters were prioritized over emission parameters. The weighting and importance values used in each scenario are presented in Table 15.

In the multi-objective optimization process, target functions were defined to enhance engine performance while reducing emissions. Accordingly, BSFC and emission parameters (NO_x, CO_2, HC, and CO) were minimized, whereas BTE was maximized. This RSM-based optimization approach enabled the identification of optimal engine operating conditions and provided a balanced evaluation of emission reduction and performance improvement.

Table 15. Optimization process

		Scenarios 1		Scenarios 2		Scenarios 3	
Response	**Goal**	**Weight**	**Importance**	**Weight**	**Importance**	**Weight**	**Importance**
BTE (%)	Maximum	1	3	1	1	1	3
BSFC (g/kWh)	Minimum	1	3	1	1	1	3
NO_x (ppm)	Minimum	1	3	1	3	1	1
CO_2 (%)	Minimum	1	3	1	3	1	1
HC (ppm)	Minimum	1	3	1	3	1	1
CO (%)	Minimum	1	3	1	3	1	1

In Figure 12, the optimization graph is displayed. The optimization study's optimal value was established at a load of 1451.71 W using test fuel that contained 9.22% biodiesel by volume to diesel. Table 15 displays the output parameter values at these ideal values. At the optimum operating condition, the fuel blend containing 9.22% cottonseed biodiesel at 1451.71 W engine load exhibited CO, HC, CO_2, and NO_x emissions of 0.028%, 20.84 ppm, 5.27%, and 633.69 ppm, respectively. Correspondingly, the BSFC and BTE values were obtained as 411.41 g/kWh and 19.87%, respectively, indicating efficient engine performance with acceptable emission levels.

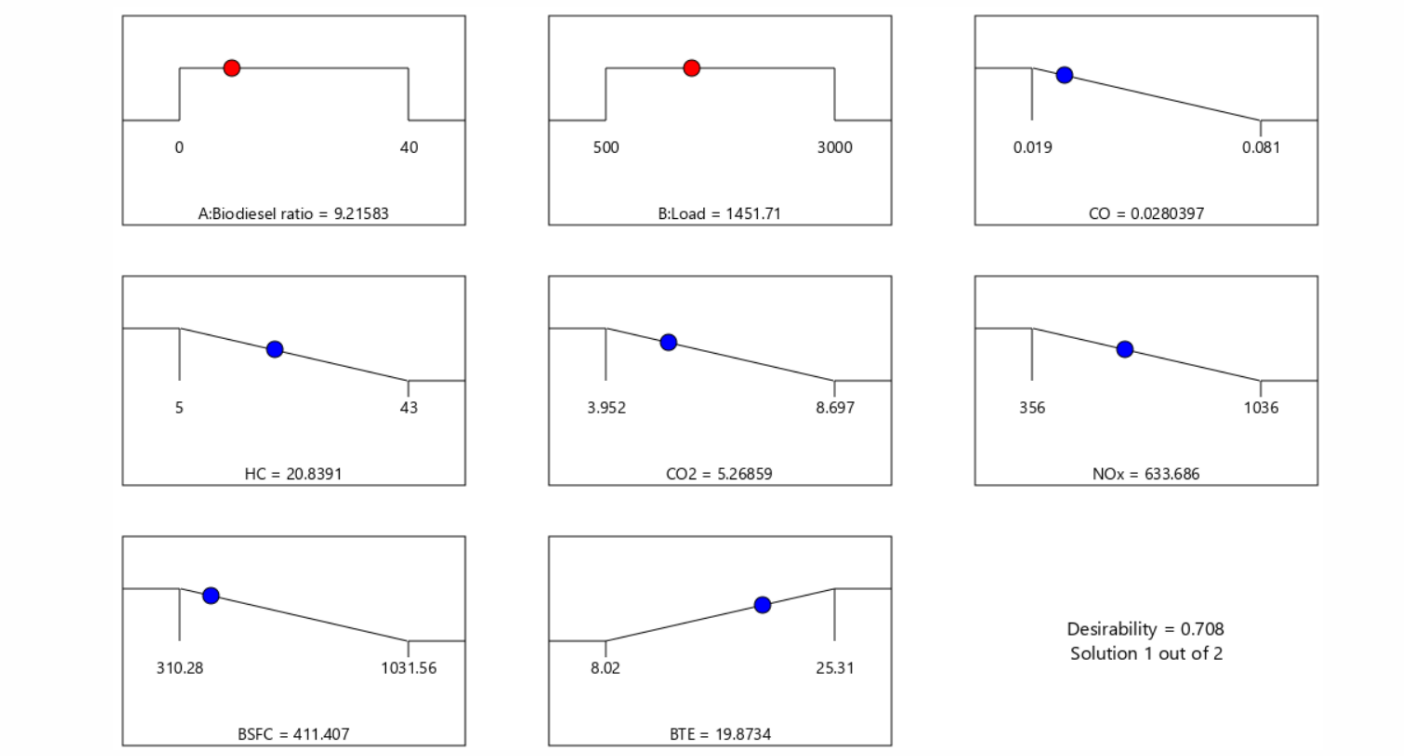


Figure 12. Optimization graph of Model 1

In Figure 13, the optimization graph of Model 2 is displayed. The optimization study's optimal value was established at a load of 1134.97 W using test fuel that contained 13.51% biodiesel by volume to diesel. Model 2 (Table 15) displays the output parameter values at these ideal values. At the optimum operating condition CO, HC, CO_2, and NO_x emissions of 0.0336%, 15.45 ppm, 4.91%, and 587.17 ppm, respectively. Correspondingly, the BSFC and BTE values were obtained as 537.91 g/kWh and 16.81%, respectively, indicating efficient engine performance with acceptable emission levels.

In Figure 14, the optimization graph of Model 3 is displayed. The optimization study's optimal value was established at a load of 1819.46 W using test fuel that contained 4.03% biodiesel by volume to diesel. Model 3 (Table 15) displays the output parameter values at these ideal values. At the optimum operating condition CO, HC, CO_2, and NO_x emissions of 0.0284%, 27.23 ppm, 5.75%, and 672.30 ppm, respectively. Correspondingly, the BSFC and BTE values were obtained as 310.28 g/kWh and 22.61%, respectively, indicating efficient engine performance with acceptable emission levels.

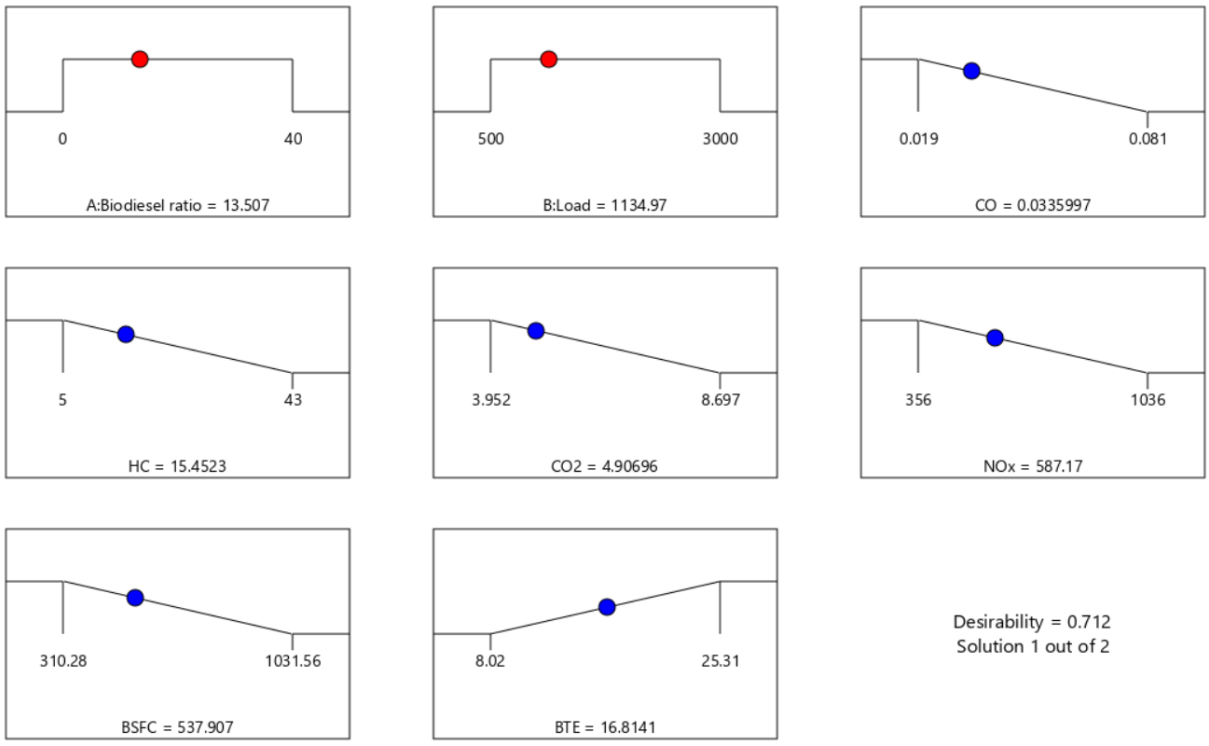


Figure 13. Optimization graph of Model 2

Table 16. Validation studies

	CO		HC		CO_2	
	Test	RSM	Test	RSM	Test	RSM
	0.028	0.0273	20	21.53	5.230	5.335
Error rates (%)	**2.59**		**7.67**		**2**	
	NO_x		**BSFC**		**BTE**	
	Test	RSM	Test	RSM	Test	RSM
	615	643	422	396.18	19.85	20.26
Error rates (%)	**4.56**		**6.12**		**2.08**	

The optimization results obtained under the three different weighting scenarios demonstrate that the optimal operating conditions vary depending on the relative importance assigned to performance and emission parameters. In Scenario 1, where equal importance was assigned to all response variables, a balanced optimization outcome was obtained, providing acceptable emission levels together with satisfactory engine performance. In Scenario 2, where emission parameters were prioritized, lower emission values were achieved; however, this scenario resulted in relatively higher BSFC and slightly lower BTE, indicating a reduction in overall engine efficiency. In contrast, Scenario 3, which prioritized performance parameters, produced the highest BTE and lowest BSFC values, but at the expense of increased emission levels.

Considering the need to simultaneously maintain engine performance and reduce exhaust emissions, Scenario 1 was considered the most appropriate optimization strategy, as it provided a more balanced trade-off between performance and emission responses. Furthermore, the variation in optimal operating conditions among the scenarios indicates that the optimization results are sensitive to the relative importance assigned to the response variables, confirming the validity of the sensitivity analysis approach. To further verify the reliability of the optimization results, an experimental validation was performed for the optimal operating conditions obtained from Scenario 1.

Validation studies were also out to assess the degree of agreement between the derived RSM results and real experimental data. Utilizing the actual experimental settings that were closest to the optimal operating conditions identified through optimization, output parameters were assessed in the validation experiments. The experimental system's limitations prevented the complete application of the ideal values; experiments were carried out at a load of 1500 W rather than 1451.71 W and with a biodiesel ratio of 9% instead of 9.22%. The regression equations provided in Table 14 were used to compute the values that the RSM anticipated for these operating conditions. The experimental findings, RSM results, and error rates are displayed in Table 16. The HC parameter had among the biggest error rate (7.67%), while the CO_2 had the least amount of errors (2%).

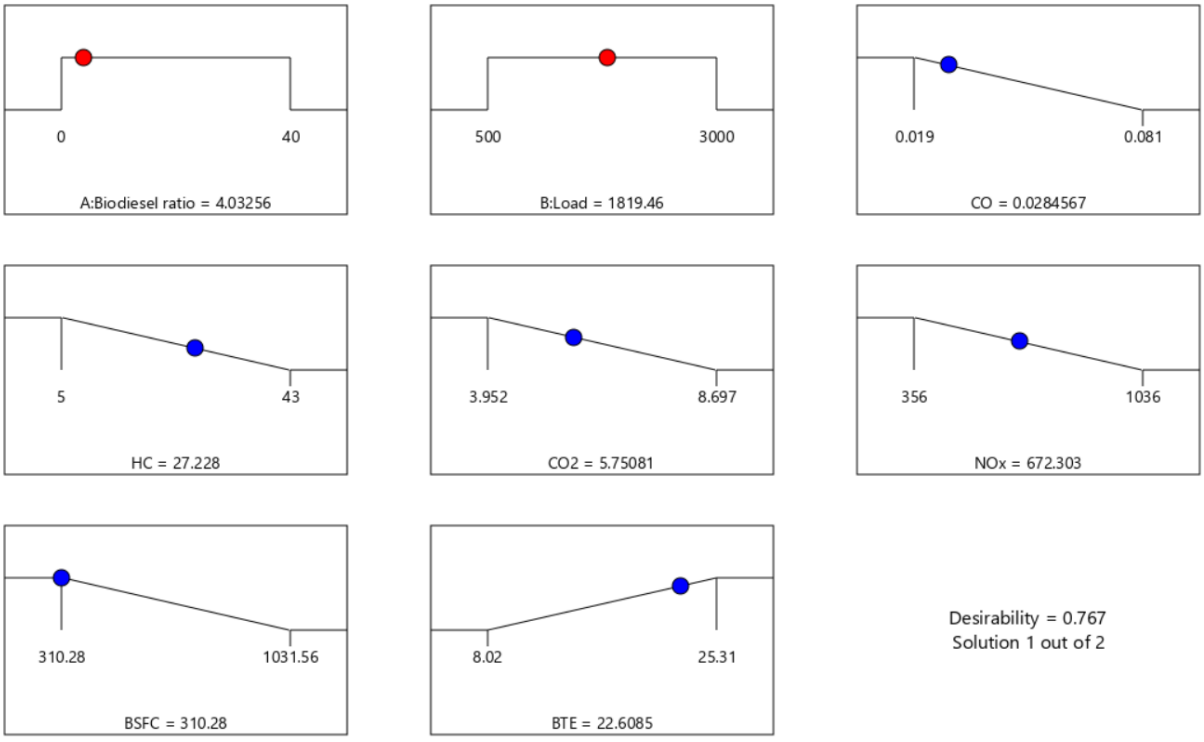


Figure 14. Optimization graph of Model 3

4. Conclusion

The present research examined the effects of adding four different volumetric ratios of cottonseed biodiesel to diesel fuel on engine performance and exhaust emissions under six different engine loads. Using RSM and the acquired experimental data, optimization was carried out to identify the ideal engine load and biodiesel blend ratio.

The emission data showed that exhaust emission characteristics were considerably influenced by engine load and the biodiesel percentage. Up to moderate blend ratios, adding biodiesel generally reduced CO and HC emissions because of its greater oxygen content and cetane number, which enhanced combustion efficiency. The C40 blend at 500 W load had the highest CO emission, 0.081%, while the C30 blend at 2500 W had the lowest, 0.025%. In the same line of thought, the C40 blend at 3000 W load displayed the highest value of 43 ppm, while the C30 mix at 500 W displayed a minimal HC emission of 5 ppm. Nevertheless, further increases in the biodiesel ratio (C40) resulted of greater CO and HC emissions due to the increased fuel viscosity and worse atomization that promoted incomplete combustion. Because of better combustion and higher in-cylinder temperature and pressure, NO_x emissions generally rose as the biodiesel ratio and engine load increased. The C30 blend had the highest NO_x emissions at 1036 ppm, while the C40 blend had the lowest at 356 ppm at 500 W load. Indicating more thorough burning, CO_2 emissions rose with increasing load and moderate biodiesel addition. They peaked at 8.697% for the C30 mix but fell to 3.962% for the C40 blend at higher biodiesel ratios where combustion efficiency declined.

The addition of biodiesel has a detrimental impact on fuel consumption and efficiency at higher blend percentages, according to engine performance findings. Because biodiesel has a higher viscosity and lower calorific value than diesel fuel, the BSFC increased as the biodiesel ratio increased. For pure diesel (C0) at 2500 W load, the lowest BSFC value was 310 g/kWh, and for the C40 blend at 500 W load, the maximum value was 1032 g/kWh. Similar to this, BTE rose for all fuels as engine load increased because of better combustion conditions, but it fell as the proportion of biodiesel grew. Pure diesel fuel produced the maximum BTE, 25%, at 2500 W load, whereas the C40 blend produced the lowest value, 8%, at 500 W load. These results show that even though biodiesel reduces emissions, adding too much of it impairs engine performance.

The resulting models' strong statistical reliability and accurate prediction of emission and performance parameters were validated by optimization and regression analysis. For CO, the reduced R^2, Adjusted R^2, and Predicted R^2 values were 92.09%, 90.83%, and 88.01%; for HC, they were 96.14%, 95.52%, and 94.39%; for NO_x, they were 94.17%, 93.49%, and 92.57%; for CO_2, they were 97.19%, 96.74%, and 96.12%; for BSFC, they were 93.51%, 92.76%, and 91.39%; and for BTE, they were

99.46%, 99.37%, and 99.26%. Strong agreement between experimental and anticipated findings is indicated by these high R^2, Adjusted R^2, and anticipated R^2 values, which also support the sufficiency and resilience of the regression models that were created. Moreover, error analysis was used to confirm the prediction accuracy. The results showed that the model prediction accuracy was adequate, with the maximum error rate for BSFC being 9.97% and the minimum error rate for BTE being 2.02%. The optimization findings showed that when emission and performance parameters were simultaneously improved, the best operating state was reached at an engine load of 1451.71 W and a biodiesel ratio of 9.22%. According to these results, low biodiesel blend ratios offer the best compromise between engine performance and emission reduction.

In conclusion, the findings unequivocally show that, especially at low and moderate blend percentages, cottonseed biodiesel may be used in diesel engines successfully without requiring any engine modification. While excessive biodiesel addition had a negative impact on performance due to its reduced calorific value and increased viscosity, blends of 10–30% biodiesel dramatically improved emission characteristics, lowering CO and HC emissions due to enhanced combustion. According to the optimization results, an engine load of 1451.71 W and a biodiesel ratio of 9.22% produced the best balance between engine performance and emission reduction, guaranteeing cleaner and more effective engine running. The trustworthiness of the generated models is confirmed by the remarkable agreement between the experimental and projected outcomes, with R^2 values up to 99.46%. These results demonstrate cottonseed biodiesel's great potential as an eco-friendly and sustainable substitute fuel for enhancing diesel engine emissions under ideal operating circumstances.

Nomenclature

BSFC	: brake specific fuel consumption
BTE	: brake thermal efficiency
CO	: carbon monoxide
CO_2	: carbon dioxide
C0	: %100 Diesel
C10	: %10 cottonseed biodiesel + %90 diesel
C20	: %20 cottonseed biodiesel + %80 diesel
C30	: %30 cottonseed biodiesel + %70 diesel
C40	: %40 cottonseed biodiesel + %60 diesel
HC	: hydrocarbon
NO_x	: nitrogen oxide
R^2	: correlation coefficient
RSM	: response surface methodology

Conflict of Interest Statement

The authors declare no conflicts of interest related to the publication of this study.

CRediT authorship contribution statement

Arif Savaş: Writing – original draft, Methodology, Software, Investigation, Conceptualization.

Samet Uslu: Writing – review & editing, Software, Methodology, Conceptualization

Declaration of Generative AI in the Writing Process

The authors stated that no AI or AI-assisted tools were utilized to prepare the study.

References

[1] Şener R. Experimental and numerical analysis of a waste cooking oil biodiesel blend used in a CI engine. International Journal of Advances in Engineering and Pure Sciences. 2021;33:299–307. https://doi.org/10.7240/jeps.829006

[2] Kalender V, Bayer MU, Yavuz M, Yilmaz IT. Techno-economic and environmental assessment of an RCCI diesel engine fuelled with fusel oil addition. Processes. 2026;14:558. https://doi.org/10.3390/pr14030558

[3] Bayer MU, Yilmaz İT, Vargün M, Kalender V, Çelik V. Investigation of the effects of hydrogen and ammonia addition on a marine auxiliary compression ignition engine. International Journal of Hydrogen Energy. 2026;216:153770. https://doi.org/10.1016/j.ijhydene.2026.153770

[4] Elkelawy M, Aly Farag M, Seleem HE. Enhancing diesel engine power plant efficiency and cutting emissions with commercial fuel additives in generator systems. Pharos Engineering Science Journal. 2025;2:37–46. https://doi.org/10.21608/pesj.2025.352985.1012

[5] Savaş A, Uslu S, Şener R. Optimization of performance and emission characteristics of a diesel engine fueled with MgCO3 nanoparticle doped second generation biodiesel from jojoba by using response surface methodology (RSM). Fuel. 2025;381:133658. https://doi.org/10.1016/j.fuel.2024.133658

[6] Savaş A, Bilgili L. Emission estimation of ship traffic in the Dardanelles. Çanakkale Onsekiz Mart University Journal of Marine Sciences and Fisheries. 2022;5:80–85. https://doi.org/10.46384/jmsf.1134339

[7] Küçüksarıyıldız H, Yaylalı Ç, Güney B. Investigation of the effect of internal combustion engine exhaust gases on workshop air quality and the importance of ventilation systems. International Journal of Automotive Science and Technology. 2025;9:618–625. https://doi.org/10.30939/ijastech..1813591

[8] Hassan QH, Al-Abboodi H. Experimental investigation of the impact of methanol-diesel blends on diesel engine emissions and performance. Combustion Engines. 2025;201(2):150–157. https://doi.org/10.19206/CE-204494

[9] Uslu S, Celik MB. Performance and exhaust emission prediction of a SI engine fueled with i-amyl alcohol-gasoline blends: An ANN coupled RSM based optimization. Fuel. 2020;265:116922. https://doi.org/10.1016/j.fuel.2019.116922

[10] Houghton-Alico D. Alcohol fuels: policies, production, and potential. Routledge; 2019.
[11] Osman AI, Nasr M, Lichtfouse E, Farghali M, Rooney DW. Hydrogen, ammonia and methanol for marine transportation. Environmental Chemistry Letters. 2024;22:2151–2158. https://doi.org/10.1007/s10311-024-01757-9
[12] Dhamodaran G, Venugopal S, Seetharaman S, Palsami T. Comparative analysis of a diesel engine fueled with hydrogen-enriched nanoparticle-emulsified second-generation biodiesel. Fuel. 2026;409:137851. https://doi.org/10.1016/j.fuel.2025.137851
[13] Rosha P, Kumar S, Senthil Kumar P, Kowthaman CN, Kumar Mohapatra S, Dhir A. Impact of compression ratio on combustion behavior of hydrogen enriched biogas-diesel operated CI engine. Fuel. 2022;310:122321. https://doi.org/10.1016/j.fuel.2021.122321
[14] Horoz E, Baydır ŞA. Engine speed-dependent NOx reduction behavior of safflower-sunflower biodiesel blends in an SCR-equipped diesel engine. Engineering Perspective. 2026;6(3):331–343. https://doi.org/10.64808/engineeringperspective.1894491
[15] Celik M, Bayindirli C, İlhak Mİ. Investigation of the performance and emissions of an engine operated with CeO2 nano additive doped biodiesel. International Journal of Automotive Science and Technology. 2022;6:113–119. https://doi.org/10.30939/ijastech..1063986
[16] Celik M, Bayındırlı C, Kuş R. Experimental investigation of effect of n-hexane addition in diesel and biodiesel fuels on performance and emissions characteristics. International Journal of Automotive Science and Technology. 2023;7:118–124. https://doi.org/10.30939/ijastech..1257614
[17] Krishnan R, S KM, Paramasivam P, Ayanie AG. Investigation of bamboo biodiesel performance in variable compression ratio engines. Energy Science & Engineering. 2025;13:5465–5481. https://doi.org/10.1002/ese3.70252
[18] Zhou G, Zhao X, Zhang Z, Liu Z, Dong S, Peng Q. Performance assessment of a diesel engine fueled with biodiesel in a plateau environment. Energies. 2025;18:1955. https://doi.org/10.3390/en18081955
[19] Simsek S. Effects of biodiesel obtained from canola, safflower oils and waste oils on the engine performance and exhaust emissions. Fuel. 2020;265:117026. https://doi.org/10.1016/j.fuel.2020.117026
[20] Yasin MHM, Paruka P, Mamat R, Yusop AF, Najafi G, Alias A. Effect of low proportion palm biodiesel blend on performance, combustion and emission characteristics of a diesel engine. Energy Procedia. 2015;75:92–98. https://doi.org/10.1016/j.egypro.2015.07.145
[21] Lei T, Wang Z, Chang X, Lin L, Yan X, Sun Y, et al. Performance and emission characteristics of a diesel engine running on optimized ethyl levulinate–biodiesel–diesel blends. Energy. 2016;95:29–40. https://doi.org/10.1016/j.energy.2015.11.059
[22] Asokan MA, Senthur Prabu S, Bade PKK, Nekkanti VM, Gutta SSG. Performance, combustion and emission characteristics of juliflora biodiesel fuelled DI diesel engine. Energy. 2019;173:883–892. https://doi.org/10.1016/j.energy.2019.02.075
[23] Kumar P, Sharma MP, Dwivedi G. Impact of ternary blends of biodiesel on diesel engine performance. Egyptian Journal of Petroleum. 2016;25:255–261. https://doi.org/10.1016/j.ejpe.2015.06.010
[24] Srithar K, Arun Balasubramanian K, Pavendan V, Ashok Kumar B. Experimental investigations on mixing of two biodiesels blended with diesel as alternative fuel for diesel engines. Journal of King Saud University - Engineering Sciences. 2017;29:50–56. https://doi.org/10.1016/j.jksues.2014.04.008
[25] Ge S, Brindhadevi K, Xia C, Salah Khalifa A, Elfasakhany A, Unpaprom Y, et al. Enhancement of the combustion, performance and emission characteristics of spirulina microalgae biodiesel blends using nanoparticles. Fuel. 2022;308:121822. https://doi.org/10.1016/j.fuel.2021.121822
[26] Savaş A, Uslu S, Kaya T. From waste to clean energy: multi-objective optimization of engine efficiency and emissions using waste plastic oil. International Journal of Automotive Engineering and Technologies. 2025;14:215–228. https://doi.org/10.18245/ijaet.1691757
[27] Shehata MS, Razek SMA. Experimental investigation of diesel engine performance and emission characteristics using jojoba/diesel blend and sunflower oil. Fuel. 2011;90:886–897. https://doi.org/10.1016/j.fuel.2010.09.011
[28] Tarabet L, Loubar K, Lounici MS, Hanchi S, Tazerout M. Eucalyptus biodiesel as an alternative to diesel fuel: Preparation and tests on DI diesel engine. BioMed Research International. 2012;2012:235485. https://doi.org/10.1155/2012/235485
[29] Gumus M, Kasifoglu S. Performance and emission evaluation of a compression ignition engine using a biodiesel (apricot seed kernel oil methyl ester) and its blends with diesel fuel. Biomass and Bioenergy. 2010;34:134–139. https://doi.org/10.1016/j.biombioe.2009.10.029
[30] İlkılıç C, Çılğın E, Aydın H. Terebinth oil for biodiesel production and its diesel engine application. Journal of the Energy Institute. 2015;88:292–303. https://doi.org/10.1016/j.joei.2014.09.001
[31] Suvanjumrat C, Kongsarai K, Phong-arom P, Chumphong N, Promtong M, Priyadumkol J. Development and optimization of an electrohydrodynamic dehydrator using ANN-GA for improved energy performance. Results in Engineering. 2025;27:106049. https://doi.org/10.1016/j.rineng.2025.106049
[32] Ajith BS, Manjunath Patel GC, Der O, Selvan CP, Samuel OD, Annadurai S, et al. Microwave-assisted transesterification of hybrid Garcinia gummi-gutta and Garcinia indica oils: Optimization using RSM and meta-heuristic algorithms for high-yield biodiesel production. Biomass and Bioenergy. 2025;202:108223. https://doi.org/10.1016/j.biombioe.2025.108223
[33] Kumaran P, Natarajan S, Kumar SMP, Rashid M, Nithish S. Optimization of diesel engine performance and emissions characteristics with tomato seed blends and EGR using response surface methodology. International Journal of Automotive

Science and Technology. 2023;7:223–233. https://doi.org/10.30939/ijastech..1326036

[34] Savaş A, Uslu S, Saral Ş. Enabling a sustainable diesel future: Emission control and performance enhancement with B2O3 nanoparticles via RSM optimization. International Journal of Automotive Science and Technology. 2025;9:174–185. https://doi.org/10.30939/ijastech..1679467

[35] Der O. Multi-output prediction and optimization of CO2 laser cutting quality in FFF-printed ASA thermoplastics using machine learning approaches. Polymers. 2025;17:1910. https://doi.org/10.3390/polym17141910

[36] Basar G, Kahraman F, Der O. Multi-response optimization of drilling parameters in direct hot-pressed Al/B4C/SiC hybrid composites using Taguchi-based Entropy–CoCoSo method. Materials. 2025;18:4319. https://doi.org/10.3390/ma18184319

[37] Mishra VK, Goswami R. A review of production, properties and advantages of biodiesel. Biofuels. 2018;9:273–289. https://doi.org/10.1080/17597269.2017.1336350

[38] Eryilmaz T, Yesilyurt MK, Cesur C, Gokdogan O. Biodiesel production potential from oil seeds in Turkey. Renewable and Sustainable Energy Reviews. 2016;58:842–851. https://doi.org/10.1016/j.rser.2015.12.172

[39] Riaz T, Iqbal MW, Mahmood S, Yasmin I, Leghari AA, Rehman A, et al. Cottonseed oil: A review of extraction techniques, physicochemical, functional, and nutritional properties. Critical Reviews in Food Science and Nutrition. 2023;63:1219–1237. https://doi.org/10.1080/10408398.2021.1963206

[40] Mohamad M, Ngadi N, Wong SL, Jusoh M, Yahya NY. Prediction of biodiesel yield during transesterification process using response surface methodology. Fuel. 2017;190:104–112. https://doi.org/10.1016/j.fuel.2016.10.123

[41] Yuksel S, Sirin TB, Ay M, Uçar M, Kurt M. A study on end mill tool geometry parameters for end milling of 316L: finite element analysis and response surface methodology optimization based on resultant cutting force. Journal of the Brazilian Society of Mechanical Sciences and Engineering. 2024;46:452. https://doi.org/10.1007/s40430-024-05027-1

[42] Canan A. Multi-purpose optimization with response surface methodology of plastic waste cables to clean energy with graphene nanoparticles. Journal of Environmental Management. 2025;391:126336. https://doi.org/10.1016/j.jenvman.2025.126336

[43] Şirin TB, Der O, Kuş H, Avdan ÇG, Yüksel S, Etyemez A, et al. Optimization of end mill geometry for machining 1.2379 cold-work tool steel through hybrid RSM-ANN-GA coupled FEA approach. Machines. 2025;14:15. https://doi.org/10.3390/machines14010015

[44] Savaş A, Uslu S, Erorhan N. Next-generation cleaner and efficient diesel operation with Mn2O3 nanoparticles: Experimental insights and multiobjective RSM optimization. Next Energy. 2026;12:100630. https://doi.org/10.1016/j.nxener.2026.100630

[45] Zhang Z, Wang T, Jia M, Wei Q, Meng X, Shu G. Combustion and particle number emissions of a direct injection spark ignition engine operating on ethanol/gasoline and n-butanol/gasoline blends with exhaust gas recirculation. Fuel. 2014;130:177–188. https://doi.org/10.1016/j.fuel.2014.04.052

[46] Panchasara H, Ashwath N. Effects of pyrolysis bio-oils on fuel atomisation: A review. Energies. 2021;14:794. https://doi.org/10.3390/en14040794

[47] Liu Z, Li S, Zhang J, Wang Y, Dai Y, Niu L, et al. Solid fuel emissions of CO pollutants in iron ore sintering process: Generation, control, and challenges. Steel Research International. 2025. https://doi.org/10.1002/srin.202500677

[48] Mofijur M, Ahmed SF, Ahmed B, Mehnaz T, Mehejabin F, Shome S, et al. Impact of nanoparticle-based fuel additives on biodiesel combustion: An analysis of fuel properties, engine performance, emissions, and combustion characteristics. Energy Conversion and Management: X. 2024;21:100515. https://doi.org/10.1016/j.ecmx.2023.100515

[49] Li R, Wang Z, Ni P, Zhao Y, Li M, Li L. Effects of cetane number improvers on the performance of diesel engine fuelled with methanol/biodiesel blend. Fuel. 2014;128:180–187. https://doi.org/10.1016/j.fuel.2014.03.011

[50] Koç MA, Şener R. Prediction of emission and performance characteristics of reactivity-controlled compression ignition engine with the intelligent software based on adaptive neural-fuzzy and neural-network. Journal of Cleaner Production. 2021;318:128642. https://doi.org/10.1016/j.jclepro.2021.128642

[51] Kumar M, Ansari NA, Gautam R. Optimising CRDI engine performance using waste-derived biodiesel, bioethanol, and ceric oxide nanoparticles: An RSM approach for emission reduction and economic viability. Fuel. 2026;415:138435. https://doi.org/10.1016/j.fuel.2026.138435

[52] Tüccar G, Tosun E, Uludamar E. Investigations of effects of density and viscosity of diesel and biodiesel fuels on NOx and other emission formations. Academic Platform Journal of Engineering and Science. 2018;6:81–85. https://doi.org/10.21541/apjes.371015

[53] Savaş A, Şener R, Uslu S, Der O. Experimental study on performance and emission optimization of MgO nanoparticle-enriched 2nd generation biodiesel: A method for employing nanoparticles to improve cleaner diesel combustion. Journal of the Energy Institute. 2025;120:102024. https://doi.org/10.1016/j.joei.2025.102024

[54] Venkatesan SP, Rahul R, Sabbharishi V, Purusothamand M, Ganesan S. Study of emission characteristics of a diesel engine run by fuel blends of diesel, jatropha biodiesel and cetane improver. Materials Today: Proceedings. 2023. https://doi.org/10.1016/j.matpr.2023.02.404

[55] Nanda Behera B, Kumar Hotta T. Influence of copper oxide nanoparticles on the performance, emission, and combustion measures of a VCR engine using palm biodiesel blended with n-butanol: A combined experimental and ANN-GA-based study. Fuel. 2025;381:133504. https://doi.org/10.1016/j.fuel.2024.133504

[56] Dere C, Deniz C. Effect analysis on energy efficiency enhancement of controlled cylinder liner temperatures in marine diesel engines with model based approach. Energy Conversion and Management. 2020;220:113015. https://doi.org/10.1016/j.enconman.2020.113015

[57] El-Shafay AS, Ağbulut Ü, Attia E-A, Touileb KL, Gad MS. Waste to energy: Production of poultry-based fat biodiesel and experimental assessment of its usability on engine behaviors. Energy. 2023;262:125457. https://doi.org/10.1016/j.energy.2022.125457

[58] Sarıdemir S, Etem Gürel A, Ağbulut Ü, Bakan F. Investigating the role of fuel injection pressure change on performance characteristics of a DI-CI engine fuelled with methyl ester. Fuel. 2020;271:117634. https://doi.org/10.1016/j.fuel.2020.117634

[59] Afzal A, Soudagar MEM, Belhocine A, Kareemullah M, Hossain N, Alshahrani S, et al. Thermal performance of compression ignition engine using high content biodiesels: A comparative study with diesel fuel. Sustainability. 2021;13:7688. https://doi.org/10.3390/su13147688

[60] Feng Z, Zhang J, Gu J, Leng X, He Z, Nishida K. Improving biodiesel atomization performance in CI engines: A review of spray behavior, droplet impingement, and advanced techniques. Processes. 2025;13:2527. https://doi.org/10.3390/pr13082527